Received 21 October 2021; revised 13 December 2021; accepted 11 February 2022. Date of publication 16 February 2022; date of current version 3 March 2022.
The review of this article was arranged by Editor X. Guo.

Digital Object Identifier 10.1109/JEDS.2022.3151850

Low-Resistive Source/Drain Formation Using Nitrogen Plasma Treatment in Self-Aligned In-Ga-Zn-Sn-O Thin-Film Transistors

HIROSHI TSUJI [1] (Member, IEEE), TATSUYA TAKEI [1], MOTOTAKA OCHI [2], MASASHI MIYAKAWA [1], KOHEI NISHIYAMA [2], YOSHIKI NAKAJIMA [1], AND MITSURU NAKATA [1]

1 Science and Technology Research Laboratories, Japan Broadcasting Corporation, Tokyo 157-8510, Japan
2 Applied Physics Research Laboratory, Kobe Steel, Ltd., Hyogo 651-2271, Japan

CORRESPONDING AUTHOR: H. TSUJI (e-mail: tsuji.h-hi@nhk.or.jp)

ABSTRACT In this work, we demonstrate the effectiveness of nitrogen plasma treatment on the formation of low-resistive source/drain (S/D) in self-aligned (SA) oxide thin-film transistors (TFTs) using a high-mobility oxide semiconductor (OS), In-Ga-Zn-Sn-O (IGZTO). The nitrogen plasma treatment was more effective at reducing the sheet resistance (R_{sheet}) of IGZTO films than the commonly used argon plasma treatment. Furthermore, R_{sheet} for nitrogen-plasma-treated IGZTO films remained low, even when the RF power and radiation time during the plasma treatment were increased when the minimum R_{sheet} was achieved. The same trends were also observed in OS films with different compositions, such as In-Ga-Zn-O and In-Sn-Zn-O. These results indicate that nitrogen plasma treatment is effective for achieving a reduction of R_{sheet} for various OS films with a wide process window regarding plasma processing parameters. The advantages could be attributed to the smaller sputtering effect on the OS films due to the lower mass of nitrogen ions than argon ions, which was verified by X-ray reflectivity and X-ray photoelectron spectroscopy analyses. For further validation, SA IGZTO TFTs with a channel length (L) of 3 to 100 μm were fabricated with nitrogen or argon plasma treatment. The width-normalized parasitic SD resistance ($R_{SD}W$) with the nitrogen plasma treatment was determined to be 11.3 Ω·cm, which was *ca.* 40% lower than that with the argon plasma treatment. This improvement in $R_{SD}W$ resulted in higher mobility (μ) in the nitrogen-plasma-treated SA IGZTO TFTs. A nitrogen-plasma-treated SA IGZTO TFT with $L = 10$ μm exhibited a high μ of 27.2 cm^2/Vs.

INDEX TERMS Thin-film transistor, self-aligned process, nitrogen plasma, argon plasma, parasitic resistance, parasitic capacitance, oxide semiconductor, In-Ga-Zn-Sn-O, In-Ga-Zn-O, In-Sn-Zn-O.

I. INTRODUCTION

Thin-film transistors (TFTs) that utilize an oxide semiconductor (OS) such as In-Ga-Zn-O (IGZO) [1], [2] have been widely investigated because of their high mobility, low off-current, low-temperature fabrication process, and applicability to large-area production. The conventional etch-stop (ES) structure of oxide TFTs suffers from a large parasitic capacitance and a long channel length due to the alignment margin of the ES layer [3], [4]. These drawbacks can be overcome by the adoption of a self-aligned (SA) structure, which is fabricated by selectively reducing the resistance of the OS film using the gate electrode as a mask. The low-resistance regions of the OS film are used as source/drain (S/D) regions. Consequently, the parasitic capacitance can be minimized because there is no overlap between the gate electrode and S/D regions in the SA structure. Furthermore, the channel length can be shortened to the length of the gate electrode [5]. These advantages make SA oxide TFTs suitable for high-speed driving devices, which are necessary in such demanding applications as large-screen high-definition organic light-emitting diode displays [6].

One of the major challenges in the fabrication of SA oxide TFTs is to form low-resistive S/D regions. Several methods have been proposed to reduce the resistance of the S/D regions using plasma treatment [7]–[10], aluminum reaction [11], [12], ion implantation [13], [14], or laser irradiation [15], [16]. Among these, plasma treatment can be most readily inserted into the process flow for oxide TFTs. Here, we investigated the effects of plasma treatment on the formation of low-resistive S/D regions in SA oxide TFTs using a high-mobility oxide semiconductor, In-Ga-Zn-Sn-O (IGZTO) [17], [18]. Argon plasma treatment is commonly used to reduce the resistance of OS films [7]; however, it unavoidably etches OS films due to the large mass of argon ions [10], which leads to an increase in the resistance. Therefore, nitrogen plasma [8], [9] was used in the present work because of the smaller mass of nitrogen ions. Nitrogen plasma treatment is expected to be effective at reducing the resistance of various OS films including IGZTO without etching them, which would offer a wide process window regarding plasma processing parameters.

II. EXPERIMENTAL DETAILS

To investigate the effects of plasma treatment on various OS films, 15-nm-thick IGZTO, IGZO, and In-Sn-Zn-O (ITZO) [19] films were deposited on glass substrates by sputtering. The sputtering conditions for each material were as follows. An Ar/O_2 gas mixing ratio of 21/9, a DC power of 120 W, a chamber pressure of 0.13 Pa for IGZTO, an Ar/O_2 gas mixing ratio of 19.4/0.6, an RF power of 100 W, a chamber pressure of 0.4 Pa for IGZO, and an Ar/O_2 gas mixing ratio of 38/2, a DC power of 300 W, a chamber pressure of 0.2 Pa for ITZO. Argon or nitrogen plasma treatment was then performed after the films were annealed at 300 °C for 1 h in air. The plasma treatment was performed using a parallel-plate reactive ion etching system with different RF power levels and radiation times. The sheet resistance (R_{sheet}) of the plasma-treated films was then measured using the four-point probe method.

Top-gate SA IGZTO TFTs were fabricated as follows. After formation of a SiO_2 underlayer on a glass substrate, an IGZTO film was deposited by sputtering at room temperature with an IGZTO target, the composition of which was optimized so that high-mobility TFTs were obtained [17]. After the IGZTO film was patterned, it was annealed at 300 °C for 1 h in air. A SiO_2 gate insulator (GI) film was then deposited by plasma-enhanced chemical vapor deposition (PECVD) at 300 °C. The thickness of the GI film was 140 nm. A Mo-alloy gate electrode was then formed. The GI film was patterned by dry etching to expose the IGZTO surface to plasma. Nitrogen or argon plasma treatment was conducted using the gate electrode as a mask to form low-resistive S/D regions. A SiO_2 interlayer was then deposited by PECVD at 200 °C. After the formation of contact holes, Mo-alloy S/D electrodes were formed.

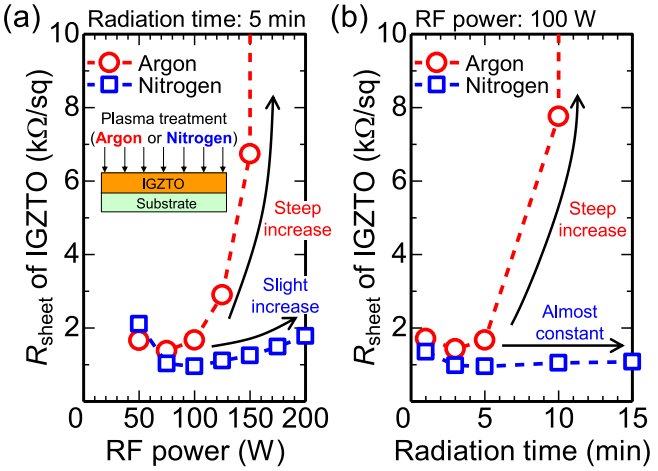

FIGURE 1. Sheet resistance (R_{sheet}) of 15-nm-thick IGZTO films treated with argon or nitrogen plasma as a function of (a) RF power and (b) radiation time. The radiation time was fixed at 5 min in (a), and the RF power was fixed at 100 W in (b).

III. RESULTS AND DISCUSSION

Figure 1 shows R_{sheet} for the IGZTO films treated with argon or nitrogen plasma as a function of (a) RF power and (b) radiation time. The radiation time was fixed at 5 min in Fig. 1(a), while the RF power was fixed at 100 W in Fig. 1(b). R_{sheet} for the IGZTO films was more than 10^8 Ω/sq without plasma treatment, whereas it was substantially reduced by the argon or nitrogen plasma treatment. However, as the plasma RF power or radiation time was increased to more than 100 W or 5 min, respectively, R_{sheet} for the argon-plasma-treated IGZTO films increased steeply. This could be attributed to a sputtering effect due to the large mass of argon ions [10]. On the other hand, R_{sheet} for the nitrogen-plasma-treated IGZTO films increased only slightly with increasing RF power, as shown in Fig. 1(a), and it was almost independent of the radiation time, as shown in Fig. 1(b). Therefore, R_{sheet} remained low, unlike that for the case of argon plasma treatment, even when the RF power and radiation time were increased. In addition, the minimum R_{sheet} (R_{min}) for nitrogen plasma treatment was 0.95 kΩ/sq, which was more than 30% lower than that for argon plasma treatment (1.38 kΩ/sq).

To further investigate the effects of nitrogen plasma treatment, OS films with different compositions, IGZO and ITZO films were also evaluated. Figure 2 shows R_{sheet} normalized with respect to R_{min} for the IGZTO, IGZO, and ITZO films treated with nitrogen plasma as a function of (a) RF power and (b) radiation time. R_{min} for the IGZO and ITZO films was 1.67 and 1.03 kΩ/sq, respectively. The same trend as that for IGZTO was observed for IGZO and ITZO; there was only a slight increase in the normalized R_{sheet} with increasing RF power, as shown in Fig. 2(a), and it was almost constant, regardless of the radiation time, as shown in Fig. 2(b). These results indicate that the nitrogen plasma treatment has high tolerance to variations in the plasma processing parameters, i.e., RF power and radiation time, which leads to a

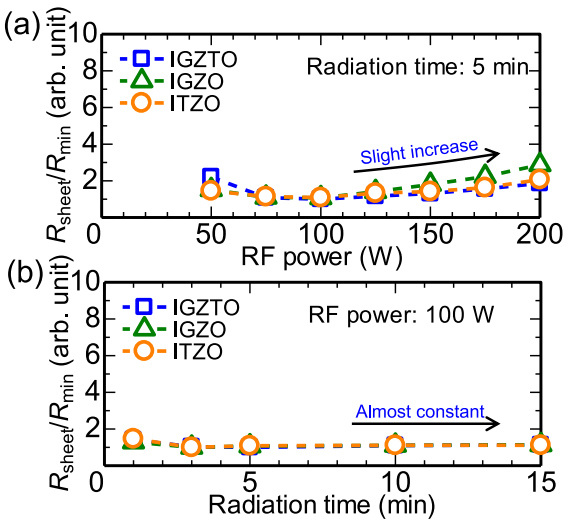

FIGURE 2. Sheet resistance (R_{sheet}) normalized with respect to the minimum resistance (R_{min}) for 15-nm-thick IGZTO, IGZO, and ITZO films treated with nitrogen plasma as a function of (a) RF power and (b) radiation time.

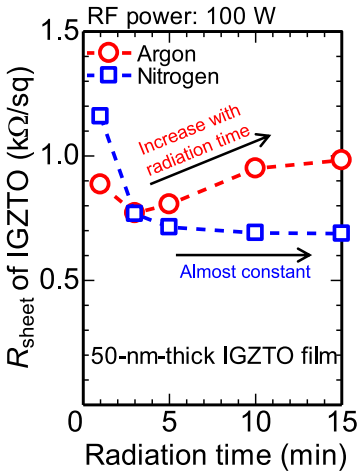

FIGURE 3. Sheet resistance (R_{sheet}) of 50-nm-thick IGZTO films treated with argon or nitrogen plasma as a function of radiation time. The RF power was fixed at 100 W.

wide process window to reduce the resistance of various OS films.

In addition, we also evaluated R_{sheet} using thick films (50-nm-thick IGZTO films) as shown in Fig. 3. Similar trends as observed for the ultrathin films (15-nm-thick IGZTO films) shown in Fig. 1 were found for the thick films: R_{sheet} for the argon-plasma-treated IGZTO films increased with increasing radiation time although R_{sheet} for the nitrogen-plasma-treated IGZTO films was almost constant once it was reduced to its minimum value (~0.7 kΩ/sq). Therefore, nitrogen plasma treatment is effective even for thick OS films.

Figure 4 illustrates a possible mechanism to explain the difference between the argon and nitrogen plasma treatment. In the case of argon plasma (Fig. 4(a)), not only oxygen

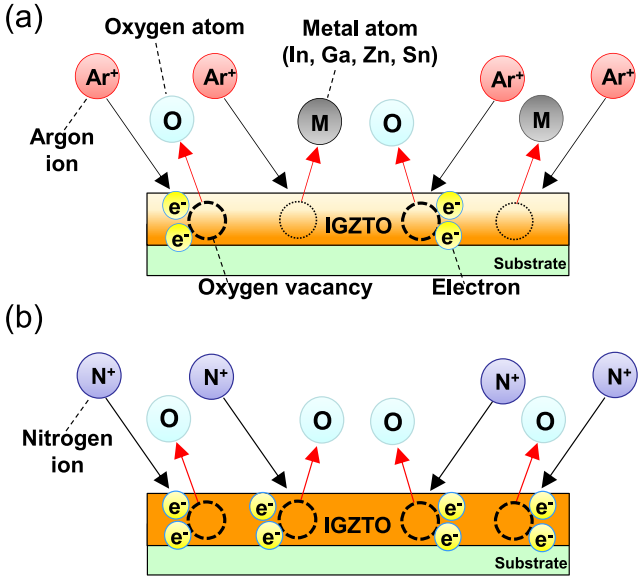

FIGURE 4. Possible mechanism to explain the difference between (a) argon and (b) nitrogen plasma treatment.

atoms, but also metal atoms such as indium, gallium, zinc, or tin atoms are sputtered because of the large mass of argon ions. Although oxygen vacancies, which act as a source of electrons [20], are formed, the IGZTO films are consequently sputtered with increasing plasma RF power and radiation time, which results in an increase in R_{sheet}, as shown in Fig. 1. On the other hand, in the case of nitrogen plasma (Fig. 4(b)), only oxygen atoms are likely to be sputtered, and not metal atoms, due to the smaller mass of nitrogen ions. Therefore, the IGZTO films are not significantly sputtered, and thus R_{sheet} remains low, even if the RF power and radiation time are increased, as shown in Fig. 1. This mechanism would be the same for other OS films, including IGZO and ITZO films, which explains the results shown in Fig. 2.

X-ray reflectivity (XRR) and X-ray photoelectron spectroscopy (XPS) analyses were performed to verify the proposed mechanism. First, to compare the sputtering effects of argon and nitrogen plasma, the film density (D_f) at the surface of the IGZTO films was determined by XRR, as shown in Table 1. D_f without plasma treatment was 6.7 g/cm^3, which was reduced to 3.5 g/cm^3 after argon plasma treatment with an RF power of 100 W and a radiation time of 10 min. On the other hand, D_f was 4.0 g/cm^3 after nitrogen plasma treatment. This confirms that IGZTO films are sputtered less by nitrogen plasma than by argon plasma, and this is considered to be due to the smaller mass of nitrogen ions. Note that the film thickness was unchanged after the plasma treatment although D_f was reduced. Therefore, it is considered that the main mechanism for the increase in R_{sheet} is related to a reduction not in the film thickness but in D_f. We also investigated the depth profiles of oxygen vacancies in IGZTO films using XPS, and the results are shown in Fig. 5. The XPS

TABLE 1. IGZTO film density (D_f) determined by X-ray reflectivity analysis.

Plasma treatment	IGZTO film density (D_f) at the surface (g/cm^3)
Argon plasma (100 W, 10 min)	3.5
Nitrogen plasma (100 W, 10 min)	4.0
w/o plasma treatment	6.7

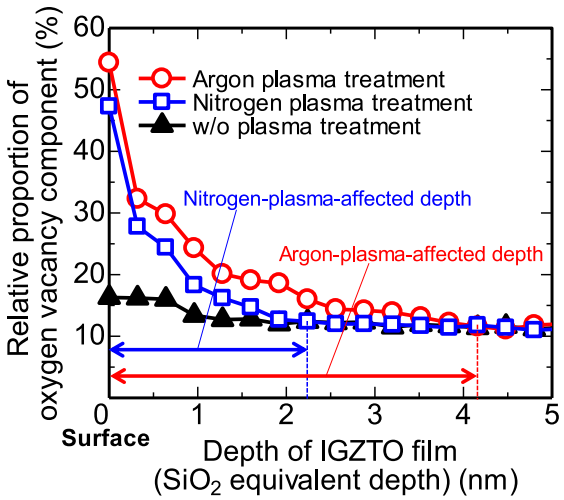

FIGURE 5. Depth profiles of relative proportion of oxygen vacancy component in IGZTO films determined by XPS analysis. The plasma RF power and radiation time were 100 W and 5 min, respectively.

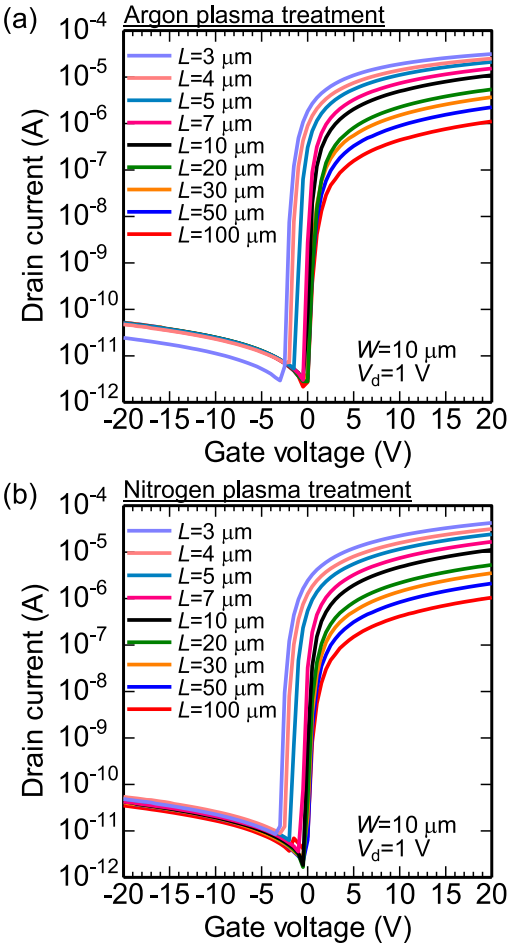

FIGURE 6. Transfer characteristics of SA IGZTO TFTs with various channel lengths (L) fabricated with (a) argon and (b) nitrogen plasma treatment. W is the channel width and V_d is the drain voltage.

analysis was performed using C_{60} ion sputtering to minimize sputtering damage [21] instead of conventional Ar ion sputtering. The depth profiles were obtained by repeatedly etching the surface using C_{60} ion sputtering. The etching rate was 1.6 nm/min. The relative proportion of oxygen vacancies was obtained from XPS O 1s spectra [10]. The nitrogen- and argon-plasma-affected depths were 2.2 and 4.2 nm, respectively. This indicates that the depth affected by nitrogen plasma is only half that for argon plasma, although nitrogen plasma enables lower resistivity, as shown in Fig. 1. Although this can be attributed to the higher D_f for the nitrogen-plasma-treated IGZTO films as shown in Table 1, further investigation is required to determine the detailed mechanism.

Figure 6 shows the transfer characteristics of SA IGZTO TFTs fabricated with (a) argon and (b) nitrogen plasma treatment. The channel length (L) for the fabricated TFTs was in the range of 3 to 100 μm and the channel width (W) was 10 μm. The RF power and radiation time used for the plasma treatment were optimized from Fig. 1 to obtain the lowest resistance for each plasma condition: 100 W and 3 min for argon plasma, and 100 W and 5 min for nitrogen plasma. For both the argon- and nitrogen-plasma-treated TFTs, the drain current began to increase exponentially at a gate voltage (V_g) of around 0 V when L was 10 μm or more. However, a shift of the transfer curve towards more negative gate voltages was observed in short-channel TFTs with L of 7 μm or less. This could be attributed to carrier diffusion from the SD regions into the channels [22].

Figure 7 shows the width-normalized total resistance ($R_{tot}W$) as a function of L at V_g of 10 to 20 V for the (a) argon- and (b) nitrogen-plasma-treated TFTs. For this plot, the data for the SA IGZTO TFTs with L of 10 μm or more were used to avoid the influence of the negative shift of the transfer curve shown in Fig. 6. The shrinkage of the channel length (ΔL) and the width-normalized parasitic SD resistance ($R_{SD}W$) were evaluated using a transmission line model [23], as shown in the insets of Fig. 7. Note that $R_{tot}W$ is obtained as the sum of two kinds of resistance: $R_{SD}W$, which is independent of L, and the width-normalized channel resistance ($R_{ch}W$), which is proportional to L-ΔL. Therefore, although $R_{ch}W$ is the dominant component of $R_{tot}W$ in long-channel TFTs, it decreases with decreasing L and the influence of $R_{SD}W$ becomes greater. There was no significant difference in ΔL; ΔL was estimated to be 1.82 μm and 1.75 μm for the argon- and nitrogen-plasma-treated TFTs, respectively. On the other hand, the $R_{SD}W$ value for the nitrogen-plasma-treated TFTs was 11.3 Ω·cm,

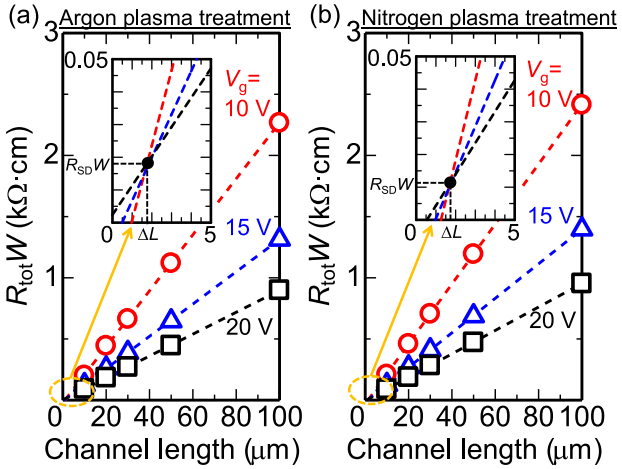

FIGURE 7. Width-normalized total resistance ($R_{tot}W$) as a function of channel length at gate voltages of 10, 15, and 20 V for SA IGZTO TFTs fabricated with (a) argon and (b) nitrogen plasma treatment. The insets show enlargements around the intersection points of the three lines. $R_{SD}W$ is the width-normalized parasitic SD resistance and ΔL is the shrinkage of the channel length.

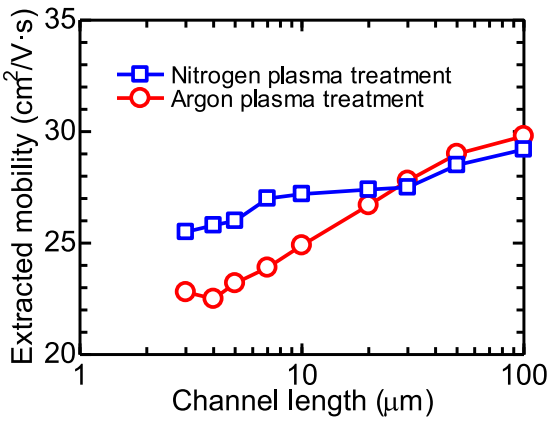

FIGURE 8. Extracted mobility as a function of channel length for SA IGZTO TFTs fabricated with argon or nitrogen plasma treatment.

which is *ca.* 40% lower than that for the argon-plasma-treated TFTs (18.1 Ω·cm). This indicates that the nitrogen plasma treatment is effective for forming low-resistive S/D regions in the SA IGZTO TFTs.

Figure 8 shows the mobility (μ) determined from the transfer curves for the SA IGZTO TFTs shown in Fig. 6, expressed as [24]:

$$\mu = g_m L / W C_{ox} V_d, \quad (1)$$

where g_m is the transconductance and C_{ox} is the gate insulator capacitance per unit area. Note that μ was determined without any correction for ΔL or the voltage drop due to the parasitic SD resistance ($R_{SD}W$). There was no significant difference in μ between the argon- and nitrogen-plasma-treated TFTs when L was 20 μm or more. However, the difference became pronounced when L was 10 μm or less; the nitrogen-plasma-treated short-channel TFTs exhibited higher μ than the argon-plasma-treated TFTs. This can be explained by the increase in the influence of the parasitic SD resistance with decreasing L [25].

TABLE 2. Electrical parameters determined for SA IGZTO TFTs (W/L = 10 μm/10 μm) fabricated with argon or nitrogen plasma treatment.

Plasma treatment	μ (cm²/V·s)	$R_{SD}W$ (Ω·cm)	ΔL (μm)	SS (V/dec)	V_{th} (V)	ΔV_{th} (V)
Argon	24.9	18.1	1.82	0.21	1.0	-1.3(NBS) 1.8(PBS)
Nitrogen	27.2	11.3	1.75	0.20	0.9	-1.3(NBS) 1.9(PBS)

Table 2 summarizes the values for the important device parameters of TFTs, i.e., μ, $R_{SD}W$, ΔL, the subthreshold swing (SS), the threshold voltage (V_{th}), and the V_{th} shift (ΔV_{th}) induced by negative and positive bias stresses (NBS and PBS). Here, V_{th} is defined as the gate voltage at a drain current of W/L×10^{-7} A. The applied gate stress voltages for NBS and PBS were −20 V and +20 V, respectively, while the stress time for both NBS and PBS was 3600 s. The nitrogen plasma treatment is superior to the argon plasma treatment in terms of μ and $R_{SD}W$. The nitrogen-plasma-treated TFT with L = 10 μm exhibited a high μ of 27.2 cm²/Vs due to a low $R_{SD}W$. However, there were no significant differences in the other parameters, including ΔV_{th}. Although it has been reported that excess nitrogen incorporation into the channel layer could degrade the electrical properties and reliability of TFTs [26], no degradation was observed, as shown in Table 2. This indicates that the nitrogen plasma treatment is effective for forming low-resistive S/D regions without the incorporation of excess nitrogen into the channel layer.

IV. CONCLUSION

The effects of nitrogen plasma treatment on the formation of low-resistive S/D regions in SA IGZTO TFTs were investigated. Compared to the commonly used argon plasma treatment, nitrogen plasma treatment was demonstrated to further reduce the resistance of IGZTO films while providing a wider processing window with respect to the plasma processing parameters. Similar trends were also observed for IGZO and ITZO films, which indicates that nitrogen plasma treatment is effective for reduction of the resistance of various types of OS films. These advantages could be attributed to lesser sputtering damage to the OS films due to the smaller mass of nitrogen ions compared to argon ions, which was verified by XRR and XPS analyses. SA IGZTO TFTs were fabricated with nitrogen or argon plasma treatment and the device characteristics were evaluated. $R_{SD}W$ obtained with the nitrogen plasma treatment was 11.3 Ω·cm, which was *ca.* 40% lower than that with the argon plasma treatment. This improvement resulted in higher μ values in the nitrogen-plasma-treated SA IGZTO TFTs. Nitrogen plasma treatment was thus determined to be effective for fabricating high-mobility SA oxide TFTs.

REFERENCES

[1] K. Nomura, H. Ohta, A. Takagi, T. Kamiya, M. Hirano, and H. Hosono, "Room-temperature fabrication of transparent flexible thin-film transistors using amorphous oxide semiconductors," *Nature*, vol. 432, pp. 488–492, Nov. 2004, doi: 10.1038/nature03090.

[2] H. Yabuta *et al.*, "High-mobility thin-film transistor with amorphous In Ga Zn O_4 channel fabricated by room temperature RF-magnetron sputtering," *Appl. Phys. Lett.*, vol. 89, pp. 1–3, Sep. 2006, doi: 10.1063/1.2353811.

[3] D. H. Kang, I. Kang, S. H. Ryu, and J. Jang, "Self-aligned coplanar a-IGZO TFTs and application to high-speed circuits," *IEEE Electron Devices Lett.*, vol. 32, no. 10, pp. 1385–1387, Oct. 2011, doi: 10.1109/LED.2011.2161568.

[4] M. Nakata, H. Tsuji, Y. Fujisaki, Y. Nakajima, T. Takei, and T. Yamamoto, "Electrical and structural characterization of self-aligned InGaZnO thin-film transistors fabricated by excimer laser irradiation," *IEEE Trans. Ind. Appl.*, vol. 53, no. 6, pp. 5972–5977, Nov./Dec. 2017, doi: 10.1109/TIA.2017.2726504.

[5] K. Myny, "The development of flexible integrated circuits based on thin-film transistors," *Nat. Electron.*, vol. 1, pp. 30–39, Jan. 2018, doi: 10.1038/s41928-017-0008-6.

[6] C. Ha *et al.*, "High reliable a-IGZO TFTs with self-aligned coplanar structure for large-sized ultrahigh-definition OLED TV," in *SID Dig.*, 2015, pp. 1020–1022, doi: 10.1002/sdtp.10346.

[7] J. Park *et al.*, "Self-aligned top-gate amorphous gallium indium zinc oxide thin film transistors," *Appl. Phys. Lett.*, vol. 93, pp. 1–3, Aug. 2008, doi: 10.1063/1.2966145.

[8] S. Chi, X. Xiao, X. He, and S. Zhang, "Self-aligned top-gate a-IGZO thin-film transistor with N_2 plasma-treated source/drain regions," in *Proc. IDW*, 2013, pp. 379–382.

[9] H. Lu, C. Ren, X. Xiao, Y. Xiao, C. Wang, and S. Zhang, "Comparison of N_2 and Ar plasma treatment for source/drain formation in self-aligned top-gate amorphous InGaZnO thin film transistor," in *Proc. 23rd Int. Workshop Active-Matrix Flatpanel Displays Devices*, Kyoto, Japan, 2016, pp. 131–134, doi: 10.1109/AM-FPD.2016.7543642.

[10] Y. Magari, H. Makino, and M. Furuta, "Carrier generation mechanism and origin of subgap states in Ar- and He-plasma-treated In-Ga-Zn-O thin films," *ECS J. Solid-State Sci. Technol.*, vol. 6, pp. Q101–Q107, Aug. 2017, doi: 10.1149/2.0031709jss.

[11] N. Morosawa, Y. Ohshima, M. Morooka, T. Arai, and T. Sasaoka, "Self-aligned top-gate oxide thin-film transistor formed by aluminum reaction method," *Jpn. J. Appl. Phys*, vol. 50, pp. 1–4, Sep. 2011, doi: 10.1143/JJAP.50.096502.

[12] T. Liang, Y. Shao, H. Lu, X. Zhou, X. Deng, and S. Zhang, "Scalability and stability enhancement in self-aligned top-gate indium- zinc-oxide TFTs with Al reacted source/drain," *IEEE J. Electron Devices Soc.*, vol. 6, pp. 680–684, 2018, doi: 10.1109/JEDS.2018.2837352.

[13] Z. Ye, L. Lu, and M. Wong, "Zinc-oxide thin-film transistor with self-aligned source/drain regions doped with implanted boron for enhanced thermal stability," *IEEE Trans. Electron Devices*, vol. 59, no. 2, pp. 393–399, Feb. 2012, doi: 10.1109/TED.2011.2175398.

[14] R. Chen, W. Zhou, M. Zhang, M. Wong, and H.-S. Kwok, "Self-aligned indium–gallium–zinc oxide thin-film transistor with phosphorus-doped source/drain regions," *IEEE Electron Device Lett.*, vol. 33, no. 8, pp. 1150–1152, Aug. 2012, doi: 10.1109/LED.2012.2201444.

[15] M. Nakata *et al.*, "Fabrication method for self-aligned bottom-gate oxide thin-film transistors by utilizing backside excimer-laser irradiation through substrate," *Appl. Phys. Lett.*, vol. 103, pp. 1–4, Oct. 2013, doi: 10.1063/1.4824301.

[16] M. Nakata *et al.*, "Development of high-mobility top-gate IGZTO-TFT and suppression of threshold voltage shift in short channel utilizing laser irradiation process," in *SID Dig.*, 2020, pp. 79–82, doi: 10.1002/sdtp.13809.

[17] M. Ochi, K. Nishiyama, Y. Teramae, H. Goto, and T. Kugimiya, "High stress stability imparted by Sn addition effect in high mobility amorphous IGZTO TFTs," in *Proc. IDW*, 2018, pp. 308–311.

[18] H. Tsuji *et al.*, "Effect of nitrogen plasma on low-resistive source/drain formation in self-aligned In-Ga-Zn-Sn-O thin-film transistors," in *Proc. IDW*, 2020, pp. 149–150.

[19] M. Nakata, C. Zhao, and J. Kanicki, "DC sputtered amorphous In–Sn–Zn–O thin-film transistors: Electrical properties and stability," *Solid-State Electron.*, vol. 116, pp. 22–29, Feb. 2016, doi: 10.1016/j.sse.2015.11.025.

[20] H. Song, G. Kang, Y. Kang, and S. Han, "The nature of the oxygen vacancy in amorphous oxide semiconductors: Shallow versus deep," *Phys. Status Solidi B*, vol. 256, pp. 1–4, Mar. 2019, doi: 10.1002/pssb.201800486.

[21] D. Sakai, N. Sanada, J. S. Hammond, and H. Iwai, "Recent developments and applications in AES and XPS," *J. Surface Anal.*, vol. 12, no. 2, pp. 97–100, 2005.

[22] D. H. Kang, J. U. Han, M. Mativenga, S. H. Ha, and J. Jang, "Threshold voltage dependence on channel length in amorphous-indium-gallium-zinc-oxide thin-film transistors," *Appl. Phys. Lett.*, vol. 102, pp. 1–4, Mar. 2013, doi: 10.1063/1.4793996.

[23] S. Martin, C.-S. Chiang, J.-Y. Nahm, T. Li, J. Kanicki, and Y. Ugai, "Influence of the amorphous silicon thickness on top gate thin-film transistor electrical performances," *Jpn. J. Appl. Phys.*, vol. 40, pp. 530–537, Feb. 2001.

[24] E. Fortunato, P. Barquinha, and R. Martins, "Oxide semiconductor thin-film transistors: A review of recent advances," *Adv. Mater.*, vol. 24, pp. 2945–2986, Jun. 2012, doi: 10.1002/adma.201103228.

[25] N. V. Duy *et al.*, "Effect of series resistance on field-effect mobility at varying channel lengths and investigation into the enhancement of source/drain metallized thin-film transistor characteristics," *Jpn. J. Appl. Phys.*, vol. 50, pp. 1–5, Feb. 2011.

[26] P.-T. Liu, C.-H. Chang, C.-S. Fuh, Y.-T. Liao, and S. M. Sze, "Effects of nitrogen on amorphous nitrogenated InGaZnO (a-IGZO:N) thin film transistors," *J. Display Technol.*, vol. 12, pp. 1070–1077, Oct. 2016, doi: 10.1109/JDT.2016.2585186.